Anal. Chem. **2004,** *76,* 3530−3535

Surface Plasmon Enhanced Diffraction for Label-Free Biosensing

Fang Yu, Shengjun Tian, Danfeng Yao, and Wolfgang Knoll*

Max-Planck-Institute for Polymer Research, Ackermannweg 10, D-55128 Mainz, Germany

Surface plasmon enhanced evanescent field at a (noble) metal/dielectric interface can be employed to enhance the diffraction efficiency of surface grating structure composed of biomolecules. Based on a Kretschmann configuration, we realized a diffraction biosensor to monitor the dynamic interaction of biological molecules in a label-free way. It was demonstrated by the binding of an anti-biotin antibody to the biotin-functionalized region of a periodically patterned surface, which generated significant optical contrast to diffract the surface plasmon field. With the aid of the synchronic surface plasmon resonance signal, a quadratic dependence of diffraction signal on the amount of bound antibody was found, which coincides with the theoretical expectation. Time-dependent measurements were conducted to estimate the density of biotin thiols on the functional region.

During the past decade, the concept of optical diffraction on periodic spatial structures has been implemented into the field of sensor development.[1−6] All of those reported strategies were based on conventional diffraction configurations in a transmission or reflection mode. The reflection mode was mostly found in biological sensing applications based on surface diffraction, whereas the transmission mode suggests absorbing materials to boost the diffraction signal,[1] which is not suitable for label-free biosensing. The concept of interface diffraction generally involves a periodic surface pattern fabricated, for example, by microcontact printing (μCP)[7] or photolithography, possessing functional and nonfunctional areas. The optical contrast modulated by the analyte binding on the functional region induces dynamic change of the diffraction efficiency, which is monitored as an output signal.

As early as 1987, our group proposed that the diffraction efficiency can be greatly enhanced by surface plasmon modes (plasmon surface polaritons, PSP).[8,9] Note, this has to be differentiated from the extensively studied approaches in which metallic gratings are used to enhance the momentum of a far-field light for surface plasmon resonance (SPR) coupling.[10,11] In our approach, the light was coupled into surface plasmon modes through a prism, and a dielectric grating fabricated on the planar metal surface was to diffract the nonradiative PSP field into the light radiation (cf. Figure 1). The grating structure with a periodicity Λ provides an additional multiple of a small momentum g with $|g| = 2\pi/\Lambda$ and delocalizes the surface plasmon field, giving rise to a typical diffraction phenomenon. The periodicity Λ is chosen to be much larger than the light wavelength, since the surface-bound electromagnetic modes can exist only in a narrow range of (ω, k) given by their dispersion behavior;[10] i.e., any scattering (or diffraction) will be an efficient process only if the final state is within the density of states accessible to surface plasmons. Therefore, one can add only a small g as "Δk" in order not to (try to) scatter the plasmon into a range in which it cannot exist, i.e., outside the angular (or momentum) range given by the width of the reflectivity curve. As a comparison to the conventional diffraction schemes, the diffraction efficiency was reported to be 6 times higher than that in the total internal reflection (TIR) configuration with the aid of the SPR enhancement, even in the case of a poor SPR coupling ($R > 0.35$).[8] The gain in diffraction efficiency represents a sensitivity enhancement for sensing applications.

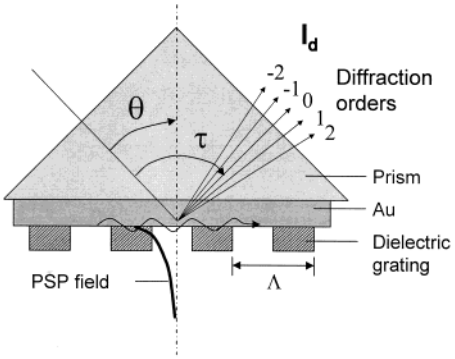

Figure 1. Schematic drawing of the diffraction sensor based on an ATR mode.

In the following, theoretical description of the surface plasmon enhanced diffraction will be briefly presented. Subsequently, the

* To whom correspondence should be addressed. E-mail: knoll@mpip-mainz.mpg.de. Phone: 0049 (6131) 379 160. Fax: 0049 (6131) 379 360.

(1) Bailey, R. C.; Hupp, J. T. *J. Am. Chem. Soc.* **2002**, *124*, 6767−6774.
(2) Nakajima, F.; Hirakawa, Y.; Kaneta, T.; Imasaka, T. *Anal. Chem.* **1999**, *71*, 2262−2265.
(3) Tsay, Y. G.; Lin, C. I.; Lee, J.; Gustafson, E. K.; Appelqvist, R.; Magginetti, P.; Norton, R.; Teng, N.; Charlton, D. *Clin. Chem.* **1991**, *37*, 1502−1505.
(4) Goh, J. B.; Loo, R. W.; McAloney, R. A.; Goh, M. C. *Anal. Bioanal. Chem.* **2002**, *374*, 54−56.
(5) John, P. M.; Davis, R.; Cady, N.; Czajka, J.; Batt, C. A.; Craighead, H. G. *Anal. Chem.* **1998**, *70*, 1108−1111.
(6) Morhard, F.; Pipper, J.; Dahint, R.; Grunze, M. *Sens. Actuators, B* **2000**, *70*, 232−242.
(7) Xia, Y.; Whitesides, G. M. *Angew. Chem., Int. Ed. Engl.* **1998**, *37*, 550−575.
(8) Rothenhäusler, B.; Knoll, W. *Opt. Commun.* **1987**, *63*, 301−304.
(9) Rothenhäusler, B.; Knoll, W. *Appl. Phys. Lett.* **1987**, *51*, 783−785.
(10) Raether, H. *Surface Plasmons on Smooth and Rough Surfaces and on Gratings*; Springer-Verlag: Berlin, 1988.
(11) Homola, J.; Koudela, I.; Yee, S. S. *Sens. Actuators, B* **1999**, *54*, 16−24.

10.1021/ac049964p CCC: $27.50
Published on Web 05/19/2004

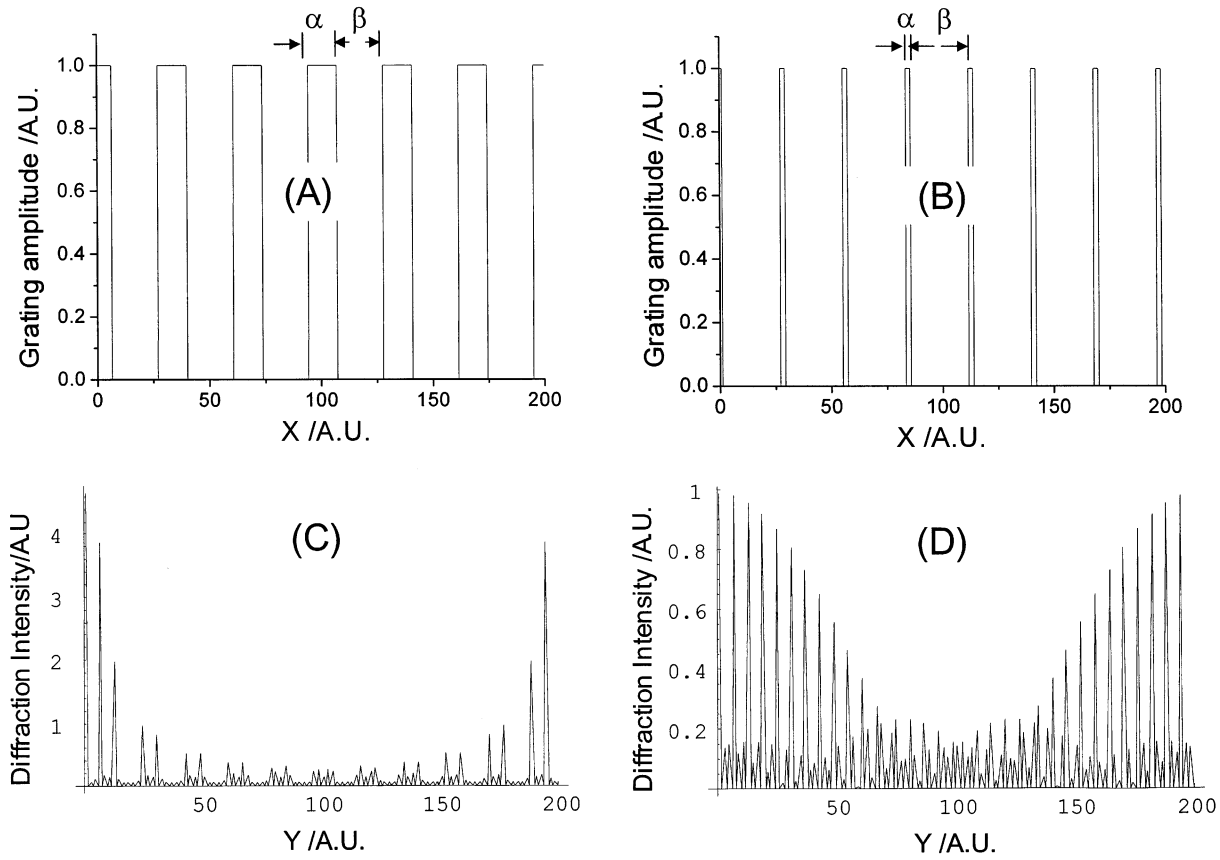

Figure 2. Simulations for the diffraction pattern of two kinds of surface periodic structures, both having the same periodicity and contrast but different line widths. The top graphs, (A) and (B), show the cross-sectional profiles of a more symmetric and an asymmetric surface periodic structure; the bottom graphs, (C) and (D), show the Fourier transforms of (A) and (B), representing their corresponding diffraction patterns and intensities.

potential biological application of this novel sensor will be demonstrated by a model system incorporating an antibody binding to a micropatterned surface.

THEORETICAL DESCRIPTION

Like the TIR diffraction mode, the ATR-based diffraction mode also allows for the observation of holographic information stored in the region of the interfacial evanescent optical field. The localized PSP wave can be diffracted by gaining (or losing) discrete momenta *mg*, which is generated by the periodic surface structure of periodicity Λ. The diffraction angle deviates in discrete increments from the specular reflection angle (i.e., zeroth-order diffraction) in fulfillment of the corresponding momentum-match condition:

$$k_{\text{diff}}^{m} = k_{\text{PSP}} \pm mg \tag{1}$$

where k_{diff}^{m} is the wavevector of the *m*th diffraction order, k_{PSP} is the wavevector the PSP wave, *g* is the grating constant with $|g|=2\pi/\Lambda$,and *m* is the diffraction order. In general, for a shallow sinusoidal grating composed of nonabsorbing materials, the diffraction intensity I_{d} can be approximated by the following expression:[12]

$$I_{\text{d}} \propto I_0(\pi \Delta nd/\lambda)^2 \tag{2}$$

where I_0 and λ are the intensity and wavelength of the source field, respectively and Δnd represents the grating amplitude in an optical thickness format. This equation conveys two important messages: (1) The diffraction intensity I_{d} is proportional to the intensity of the excitation source—the evanescent field, which emphasizes the importance of the surface plasmon field enhancement. (2) I_{d} is proportional to the square of the grating amplitude Δnd.

As indicated by Fourier diffraction optics, the diffraction pattern is a Fourier transformation of the source pattern, which can assist a proper grating design. For simplicity, patterns of repeating parallel lines were applied represented by square-wave functions. Figure 2 shows patterns A and B with the equal amplitudes and periodicities ($\Lambda = \alpha + \beta$), but different aspect ratios $\rho = \alpha/\beta$, and their corresponding Fourier transforms C and D. A symmetric pattern with ρ closer to 1 concentrates the diffracted intensity at the first several diffraction orders (cf. Figure 2C), as it resembles a sinusoidal grating and contains less frequency artifacts. For an asymmetric grating, the diffraction orders are evenly distributed (cf. Figure 2D), with the intensity being significantly reduced. Therefore, a symmetric grating pattern renders higher diffraction intensity, which generally meets the sensing demand.

EXPERIMENTAL SECTION

Materials. Biotin thiol and oligo(ethylene glycol) thiol (spacer thiol) derivatives were synthesized by Roche Diagnostics. The

(12) Nelson, K. A.; Casalegno, R.; Miller, R. J. D.; Fayer, M. D. *J. Chem. Phys.* **1982**, *77*, 1144−1152.

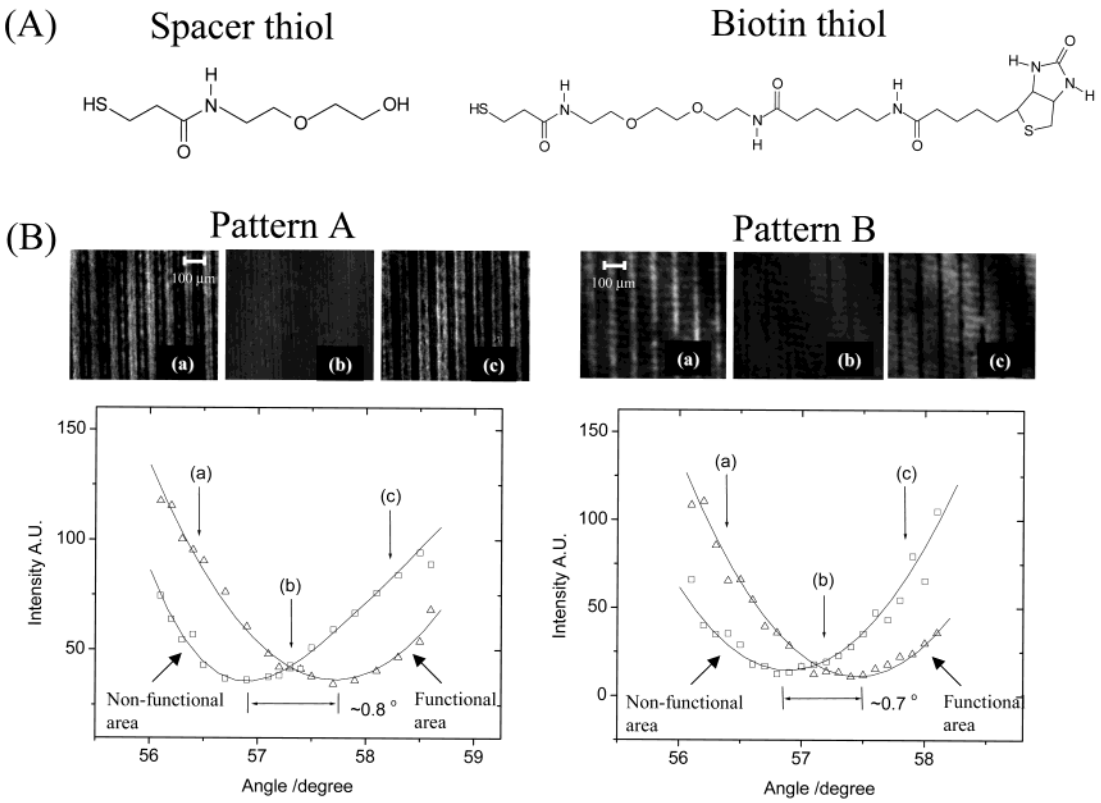

Figure 3. (A) Molecular structures of the biotin and spacer thiols used in the study. (B) SPM angular analysis for pattern A (left panel) and pattern B (right panel) treated with the anti-biotin antibody. The SPM images shown were taken near the SPR resonance angles (their corresponding angular positions are marked in the plots below, by (a), (b), and (c), with the image contrast of both functional and nonfunctional areas being reversed at the angle position of (b).

molecular structures are given in Figure 3A. Mouse anti-biotin monoclonal antibody 2F5 ($M_w \approx 150$ kDa) was purchased from Molecular Probes. D-Biotin and guanidine hydrochloride was purchased from Sigma. HBS-EP buffer (degassed 10 mM HEPES buffer saline, pH 7.4, 150 mM NaCl, 3 mM EDTA, 0.005% (v/v) surfactant P-20, Biacore, Uppsala, Sweden) was used for the preparation of the protein/biotin solutions.

μCP for Surface Patterning. Two poly(dimethylsiloxane) stamps with embossed lines were prepared using Sylgard 184 silicon elastomer (Dow Corning). The stamps shared the same periodicity $\Lambda = 100\ \mu$m, but with the embossed lines being $\alpha = 42\ \mu$m (pattern A) and $\alpha = 6\ \mu$m (pattern B) in width, respectively (the cross-sectional analysis is given in the Supporting Information). For the surface patterning, the stamp was inked for 5 min in an ethanolic solution of the mixed biotin and spacer thiol (molar ratio 1:9) with a net concentration of 0.5 mM. Excess thiol solution was removed and the stamp was dried in a flow of nitrogen. The stamp was then brought into contact with the freshly evaporated Au (50 nm) substrate for a period of 1−1.5 min. After rinsing with copious amounts of ethanol, the Au substrate was exposed to an ethanolic solution of the pure spacer thiol (2 mM) for 10 min in order to passivate the nonderivatized areas. Finally, the patterned substrate was rinsed with ethanol and dried in a flow of nitrogen. An "unpatterned" surface, as paper, means a surface completely covered by a mixed self-assembled monolayer (SAM) composed of biotin and spacer thiol with molar ratio of 1:9 unless otherwise mentioned.

Instrumental Information. The diffraction experiments were based on a Kretschmann surface plasmon resonance spectroscopy (SPR or SPS) setup, which has been described in detail elsewhere.[13] A p-polarized HeNe laser ($\lambda = 633$ nm, 5 mW) was used for the excitation of the PSP. The reflected/diffracted light was measured by a photodiode detector. For the diffraction scan, the angular acceptance $\Delta\tau$ of the detector was ~0.08°, which was limited by a 1-mm slit. The sample (prism, Au substrate, and flow cell) and the detector were mounted to two coaxial goniometers, respectively, enabling an independent tuning of the incident angle of the laser, the detection angle, or both. Both motors rotated in a $\theta/2\theta$ fashion for the SPR angular scan. For a diffraction scan, only the detector motor rotated (I_d versus τ, cf. Figure 1) while the sample motor kept static at the SPR minimum angle. Surface plasmon microscopy (SPM) measurements were conducted by expanding the laser beam and replacing the photodetector with a lens and a CCD camera. A glass flow cell was coupled to the Au surface, and a peristaltic pump delivered the sample liquid at a flow rate of 3 mL/min.

RESULTS AND DISCUSSION

Microscopic Characterization on Patterned Surfaces. An antibody monolayer was bound on the functional regions by exposing the patterned surfaces to an anti-biotin solution (20 nM). The SPM images of both pattern A and B surfaces can be seen in Figure 3. By sampling the gray scale value in a series of angular SPM images, angle−reflectivity curves equivalent to SPR were obtained for both functional and nonfunctional regions, for determining the SPR minimum angle shift $\Delta\theta$, which is propor-

(13) Yu, F.; Yao, D.; Knoll, W. *Anal. Chem.* **2003**, *75*, 2610−2617.

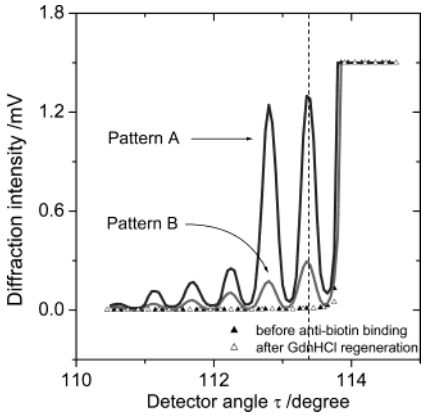

Figure 4. Diffraction angular scans obtained on the patterned surfaces with (full black and gray curves for patterns A and B, respectively) and without (full and open triangles) the binding of the anti-biotin.

tional to the grating amplitude Δnd. For patterns A and B, the $\Delta\theta$ was $\sim 0.8°$ and $\sim 0.7°$ between functional and nonfunctional areas, respectively. While on an unpatterned surface completely covered by the biotin SAM (ratio, 1:9), the binding of anti-biotin gave $\Delta\theta = 0.83° \pm 0.03°$.[13] The antibody coverage on the functional stripes of pattern A was nearly as much as that on the unpatterned surfaces. Whereas, the coverage was slightly lowered on pattern B. This could suggest a decreased molar fraction of the biotin thiolates in the functional area of pattern B (as will be discussed in the last section).

Antibody Monolayer Induced Light Diffraction. Prior to the anti-biotin binding, the optical contrasts of both patterned surfaces originated from the 10% biotin thiol (slightly larger than the spacer thiol), which were insufficient to render measurable diffractions (cf. full triangles in Figure 4). Subsequently, significant diffractions were observed upon exposing the surfaces to the antibody solution (cf. full curves in Figure 4). For pattern A, the first two observable diffraction orders had more pronounced intensities, in agreement with the simulation for a symmetric pattern (cf. Figure 2C). For pattern B, the diffraction intensity was more evenly distributed, also in agreement with the simulation for an asymmetric pattern (cf. Figure 2D). It is noteworthy that pattern A provided much stronger diffraction peaks than pattern B with the close grating amplitudes ($\Delta\theta = 0.8°$ and $0.7°$). Moreover, the bound antibodies could be completely denatured and removed from the surface by a pulse injection (<5 min) of a 4 M aqueous guanidine hydrochloride solution. Removal of the antibody reset the diffraction pattern to the original level (cf. open triangles in Figure 4). Another injection of the anti-biotin antibody resulted in identical diffraction signals, which suggests the surfaces were as ~100% functional as preregeneration (data not shown). The patterned surfaces were highly robust to sustain the regeneration condition for many times.

Quadratic Effect of Diffraction Intensity. The diffraction intensity could be monitored as a function of time, realizing a kinetic observation of biomolecular bindings. Before introducing the antibody, the incident light was set at the SPR minimum θ_0 to generate a strong PSP field. The detector arm was tuned to the diffraction peak, shown as the dashed line in Figure 4. Having a larger biotin area, the pattern A surface could give a significant SPR and diffraction signal upon antibody binding, and then a

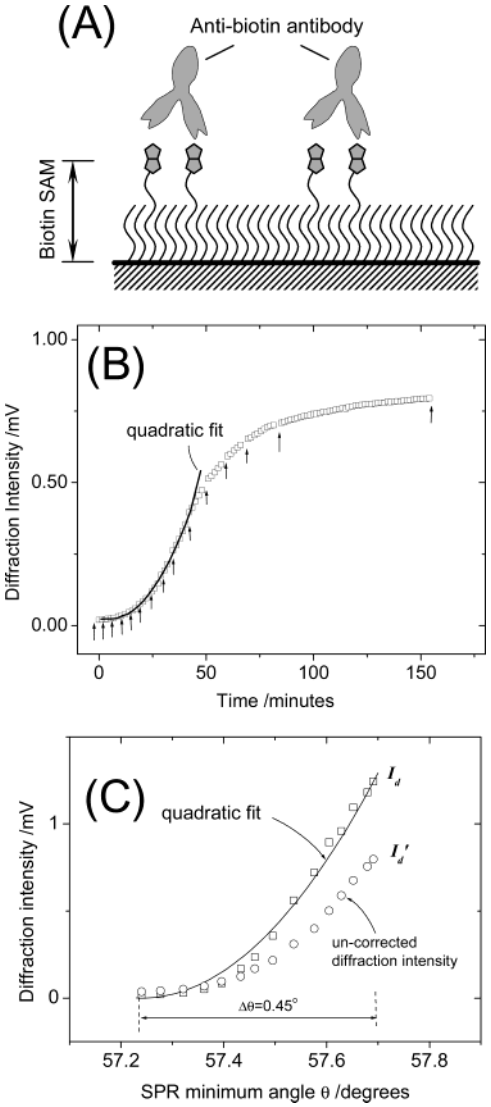

Figure 5. (A) Schematic of the biotin/anti-biotin antibody interaction model applied to reveal the quadratic effect of the diffraction signal. (B) Time-resolved diffraction signal upon the binding of anti-biotin antibodies from a 5 nM solution on the surface of pattern A. At each point indicated by an arrow, an SPR scan was performed and the diffraction signals on both the uncorrected and the corrected incident angles were obtained. The kinetic curve started with a quadratic behavior and gradually reached equilibrium due to the saturation of the surface biotin sites. (C) Corrected and uncorrected diffraction intensities versus the corresponding SPR minimum angles. (See text for details.)

relationship between both signals could be established. The working concentration of the anti-biotin solution was 5 nM, to realize a mass transport limited binding. Under such conditions, the antibody binding could be delayed for quantitative SPR/diffraction angular scans by manipulating, for example, the flow rate of the sample delivering. The following steps were performed at each point indicated in Figure 5B by an arrow: (a) The flow rate was reduced to zero, which largely ceased the antibody binding. Then a diffraction scan was preformed to get I_d'. (b) An SPR angular scan was performed to obtain the new SPR minimum angle θ. The laser incident angle was then corrected to be at the new θ, to ensure equal PSP generation. Another diffraction angular scan was performed to obtain I_d. (c) The laser incident angle was

adjusted back to the original angle θ_0 and the IgG binding kinetics continued by recovering the sample flow.

For a typical mass transport limited binding, a linear signal/time relationship is expected at the initial phase under, e.g., SPR recording.[13] However, a quasi-quadratic increase of the diffraction intensity was observed in the kinetic curve (cf. Figure 5B). This could be interpreted by the quadratic relationship between the SPR and the diffraction signals as plotted in Figure 5C. Since the SPR minimum shift is a linear reflection of the grating amplitude Δnd, the relationship coincided with the theoretical prediction (eq 2), as well as the experimental observation by another group.[14] The angular correction (step c) was found to be essential for eliminating the strong "detuning" effect of the PSP field (cf. "uncorrected curve" $I_d'-\theta$ given in Figure 5C) and eventually obtaining proper I_d values. The diffraction signal was considerably underestimated (I_d' versus I_d) if the laser incident angle was kept constant, because the SPR shifted positively up to $\Delta\theta = 0.45°$, causing a corresponding decrease of the PSP coupling efficiency ("detuning").[13] This needs to be taken into account when the analyte binding induces significant SPR shift.

Interfacial Kinetic Studies for the Estimation of the Biotin Density. It remains unclear whether the ratio of the thiolates in the stamped binary SAM is the same as that in the binary SAM prepared by dipping the Au into the thiol solution, i.e., the "normal" way. A rigorous investigation requires the involvement of surface characterization instruments such as X-ray photoelectronic spectroscopy, atomic force microscopy, etc. However, a general conclusion is still hard to draw since it may vary with different thiol couples. In the following, we attempt to get a preliminary sense of the thiol ratio by diffractive study of the interaction kinetics.

Due to the double valency of an antibody (two recognition sites per molecule), the desorption kinetics between a bound antibody and its surface-tethered antigen is strongly dependent on the surface density of the antigen, due to a 1:1−1:2 binding stoichiometry evolution.[15−17] In return, knowing the antibody desorption kinetics allows one to estimate the antigen density. To calibrate the dependence, an SPR study on a series of "unpatterned" surfaces exposing various biotin densities was conducted. The surfaces were prepared by incubating the Au substrates in mixed-thiol solutions with various molar ratios of biotin/spacer thiol from 1:9 to 1:249. The antibody solution (20 nM) was then brought into contact with the surfaces. Upon reaching binding equilibrium, the antibody was partially desorbed by rinsing with pure buffer, followed by a competitive rinse with a 1 mM biotin solution in order to rule out the influence of the rebinding effect.[15,18]

The normalized SPR desorption curves were plotted in Figure 6, for a clearer comparison of the desorption rates. In agreement with the prior work,[15] all the desorption curves had double-exponential behaviors, which made the mathematical treatment too complex to quantify the affinities. Qualitative comparison was given in this sense. For both the normal (cf. curves a in Figure 6) and the competitive (cf. curves b in Figure 6) desorbing processes, antibody desorption was faster on a SAM surface possessing a lower biotin ratio. Assuming the cross-sectional area of a thiolate is A = 0.26 nm^2 [19] and a homogeneous mixing of both thiolates, we calculated that the distance between the neighboring biotin thiolates were 1.6, 2.6, 3.6, 5.1, and 8.1 nm for 1:9, 1:24, 1:49, 1:99, and 1:249 SAM surfaces, respectively. Considering the dimension of a Fab fragment (~6.5 × 3.5 nm^2) of an IgG, these distance values could influence the probability of an antibody to bridge between two biotins. Hence, we infer that the experimental affinity evolution indicates a 1:2−1:1 transition of interaction stoichiometry between the antibody and the surface biotin, with the statistical enlargement of the biotin distance.

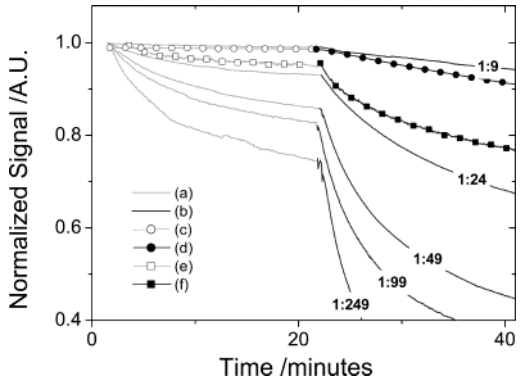

Figure 6. Normalized desorption curves for the surface biotin density determination. SPR kinetic results show the desorption (a) and competitive desorption (b) of bound anti-biotin antibody on unpatterned SAM surfaces prepared by biotin/spacer thiol mixtures with ratios of 1:9, 1:24, 1:49, 1:99, and 1:249, respectively. Curves c−f are the diffraction kinetic curves: (c) and (d) are the desorption and competitive desorption obtained on pattern A surface; (e) and (f) are the desorption and competitive desorption obtained pattern B. The diffraction intensities have been corrected by a square root conversion, considering the quadratic effect of the diffraction signal.

The aforementioned binding/desorbing/competitive desorbing process was performed on the pattern A and B surfaces, monitored by the diffraction kinetic mode. The linearized results were placed into the affinity transition curves calibrated by SPR in Figure 6. One can notice that the desorption behavior on pattern A (cf. curves c and d in Figure 6) resembled that on the 1:9 surfaces, except for a small deviation in the competitive desorption phase. This indicates that the biotin ratio on the functional areas of pattern A was close to that on an unpatterned 1:9 SAM surface. The ratio on the pattern B surface was slightly lower than that on an unpatterned 1:9 SAM surface, as was implied by the faster desorption (cf. curves e and f in Figure 6). Both observations were in agreement with the above SPM results; that is, the antibody coverage was slightly lower on pattern B than on pattern A (cf. Microscopic Characterization on Patterned Surfaces). We infer that the narrower embossed lines in stamp B (see the Supporting Information) would probably encounter a deformation during the stamping that resulted in an incomplete formation of the SAM layer on the contacting areas. The defects were subsequently filled with the spacer thiol, leading to a dilution of the biotin thiolates.

(14) Hasegawa, M.; Yamamoto, T.; Kanazawa, A.; Shiono, T.; Ikeda, T. *Chem. Mater.* **1999**, *11*, 2764−2769.
(15) Duschl, C.; Sevin-Landais, A.-F.; Vogel, H. *Biophys. J.* **1998**, *70*, 1985−1995.
(16) Bamdad, C. *Biophys. J.* **1998**, *75*, 1989−1996.
(17) Müller, K. M.; Arndt, K. M.; Plückthun, A. *Anal. Biochem.* **1998**, *261*, 149−158.
(18) Lagerholm, B. C.; Thompson, N. L. *Biophys. J.* **1998**, *74*, 1215−1228.
(19) Nelles, G.; Schönherr, H.; Jaschke, M.; Wolf, H.; Schaub, M.; Küther, J.; Tremel, W.; Bamberg, E.; Ringsdorf, H.; Butt, H.-J. *Langmuir* **1998**, *14*, 808−815.

To prove it, a systematic study is required combining with other instrumental assistance and will be the subject of another report.

CONCLUSION

This paper has briefly discussed the physical nature of the surface plasmon field enhanced diffraction sensor. This novel sensing format offered label-free and real-time observation of interfacial biomolecular interaction events, with good sensitivity and stability. Theoretical considerations from Fourier diffraction and experimental evidence showed that the pattern with an aspect ratio ρ close to 1 helped to concentrate the diffracted energy in the first several diffraction orders. It was also found theoretically and experimentally that the diffraction intensity increases quadratically with increase of the optical contrast, which implies the role of the initial contrast in achieving higher sensitivity. A technical problem, the SPR "detuning" effect, underestimated the diffraction signal to some extent when the analyte binding induced large SPR shift. An investigation on antibody desorption kinetics preliminarily revealed a nearly similar ratio of biotin/spacer thiolates on the patterned region with that on the unpatterned surface and demonstrated the applicability of this diffraction sensor in kinetic analysis.

ACKNOWLEDGMENT

We thank Roche Diagnostics for providing the thiols and the streptavidin. We thank Mr. Lau King Hang Aaron (Institute of Materials Research & Engineering (IMRE), Singapore) for his efforts in fabricating the masters by photolithography. We also acknowledge helpful discussions with Prof. Neal Armstrong (University of Arizona), and Dr. Akira Baba (University of Texas at Houston).

SUPPORTING INFORMATION AVAILABLE

Additional information as noted in text. This material is available free of charge via the Internet at http://pubs.acs.org.

Received for review January 6, 2004. Accepted March 30, 2004.

AC049964P